

## Pauli Spin and Spin-Orbit Effects in the Magnetization of a Superconducting Ti-Mo Alloy

J. A. CAPE

North American Aviation Science Center, Thousand Oaks, California

(Received 4 March 1966)

Results are given for some detailed measurements on the upper critical field  $H_{c2}$ , and on the relative slope of the magnetization curve  $\chi_s \equiv [\partial M - M_s]/\partial H]_{H_{c2}}$  for the high-field ( $\kappa_G \approx 65$ ) superconductor Ti-16 at. % Mo. The data on the temperature dependence of  $H_{c2}$  and  $\chi_s$  are shown to be in excellent agreement with recent theories in which Pauli spin paramagnetism and spin-orbit scattering have been included in Gor'kov's equations. It is observed that the  $H_{c2}$  values at  $T \ll T_{c0}$  are smaller than expected for the spin-independent case (no paramagnetic effects) and larger than expected if spin paramagnetism is allowed for but spin-orbit scattering is not. The parameter  $\kappa_2 \propto \chi_s^{-1/2}$  is found to decrease with decreasing temperature, in contrast to the case of non-"paramagnetically-limited" type-II superconductors, where  $\kappa$  is observed to increase with decreasing  $T$ . When one uses the calculated (from resistivity and specific-heat data) value of 1.75 for the Pauli spin parameter ( $\alpha = 3\hbar/2m\lambda v_F$ ), the experimental points and the theoretical curves for  $H_{c2}(T)$  are brought into excellent agreement by the proper choice of a single parameter,  $\tau_{so}$ , the phenomenological spin-orbit scattering time. For the same value of  $\tau_{so}$ , the agreement for  $\kappa_2$  is not so good. The critical-field curve cannot be fitted unless spin-orbit coupling is taken into account.

### INTRODUCTION

THE possibility that Pauli spin paramagnetism might lower a metal's normal-state free energy relative to that of its superconducting state and thereby lower the critical field for transition to the normal state was first appreciated by Clogston<sup>1</sup> and Chandrasekhar<sup>2</sup> who considered the case of superconducting filaments. Shortly thereafter Berlincourt and Hake<sup>3,4</sup> pointed out that electron spin effects had been neglected in the Gor'kov<sup>5</sup> formulation of the theory of type-II superconductors, and attributed the discrepancies between this theory and their experimental results on high-field superconducting alloys to this omission. The behavior of an ideal reversible type-II superconductor with and without spin effects is illustrated qualitatively in the free-energy and magnetization curves of Fig. 1. Maki and Tsuneto<sup>6,7</sup> and Maki<sup>8</sup> subsequently reformulated the Gor'kov equations, taking into account explicitly spin paramagnetism as well as orbital diamagnetism. This led to critical fields lower than the experimental observations, presumably—it was conjectured—because of the neglect of spin-orbit scattering. Recently, Maki<sup>9</sup> and independently Werthamer, Helfand, and Hohenberg (WHH)<sup>10</sup> have shown that the inclusion of spin-orbit scattering reduces the effect

of the Pauli term and reasonably good agreement with experiment could be attained.<sup>10</sup> Until now, the comparison of theory and experiment has been hampered by insufficient data on the electronic structure param-

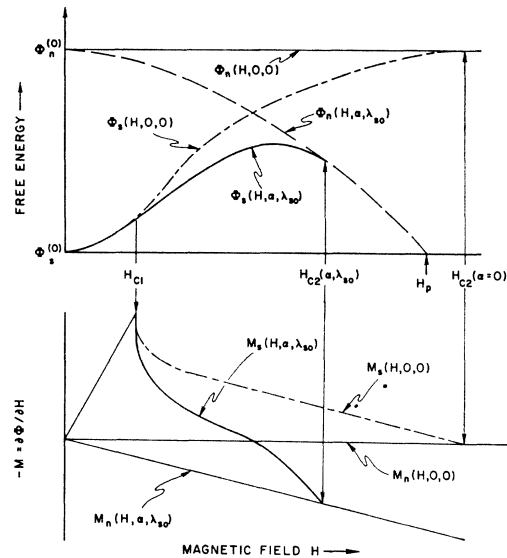


FIG. 1. Schematic of the magnetic free energies and magnetizations for the superconducting and normal states of a metal with and without electron spin effects. The curve  $\Phi_n(H, \alpha, \lambda_{so})$  represents the normal-state free energy and is parabolic so that  $M_n = \partial \Phi_n / \partial H$  is a straight line. The curve  $\Phi_s(H, \alpha, \lambda_{so})$  is the corresponding superconducting-state free energy including spin effects. The transition field  $H_{c2}(\alpha, \lambda_{so})$  to the normal state is determined by the intersection of these two curves. The intersection is drawn to suggest equal slopes [ $M_n(H_{c2}) = M_s(H_{c2})$ ], indicating, in this case, a second-order transition. The curves  $\Phi_s(H, 0, 0)$  and  $\Phi_n(H, 0, 0)$  represent the corresponding free energies of the normal and superconducting states in the absence of spin paramagnetism, and may be thought of simply as the special case  $\chi_n = \partial M_n / \partial H = 0$  ( $\alpha$  is essentially proportional to  $\chi_n$ ). One may note the familiar magnetization curve (dashed line) for this case. The Clogston critical field  $H_p$  is given by setting  $\Phi_s(H, \alpha, \lambda_{so})$  equal to  $\Phi_s(0)$  and therefore effectively ignores the field dependence of the superconducting state.

<sup>1</sup> A. M. Clogston, Phys. Rev. Letters 9, 266 (1962).  
<sup>2</sup> B. S. Chandrasekhar, Appl. Phys. Letters 1, 7 (1962).  
<sup>3</sup> T. G. Berlincourt and R. R. Hake, Phys. Rev. Letters 9, 293 (1962).  
<sup>4</sup> T. G. Berlincourt and R. R. Hake, Phys. Rev. 131, 140 (1963).  
<sup>5</sup> L. P. Gor'kov, Zh. Eksperim. i Teor. Fiz. 36, 1918 (1959); 37, 1407 (1959) [English transl.: Soviet Phys.—JETP 9, 1364 (1960); 10, 998 (1960)].  
<sup>6</sup> K. Maki and T. Tsuneto, Progr. Theoret. Phys. (Kyoto) 28, 163 (1962).  
<sup>7</sup> K. Maki and T. Tsuneto, Progr. Theoret. Phys. (Kyoto) 31, 945 (1964).  
<sup>8</sup> K. Maki, Physics 1, 127 (1964).  
<sup>9</sup> K. Maki, private communication (to be published).  
<sup>10</sup> N. R. Werthamer, E. Helfand, and P. C. Hohenberg (to be published).

eters of the alloys in question, and by insufficiently precise data on the temperature dependence of the critical fields. Accordingly, this work was undertaken to study in detail the magnetization of Ti-16 at.% Mo, an alloy for which there existed already a good deal of data on the electronic structure,<sup>11-13</sup> and on the superconductive properties.<sup>3,4,13</sup> Moreover, for this same alloy, Hake<sup>13</sup> has recently found that the high field portion of the mixed state magnetization curve lies in the paramagnetic domain, much as illustrated by the solid curve in Fig. 1.

## EXPERIMENTAL

### Magnetic Measurements

Magnetic-moment measurements were performed by means of a vibrating sample magnetometer similar to that described by Foner.<sup>14</sup> The present apparatus differs from the original Foner arrangement in that the sample is vibrated along the direction of the applied field rather than transverse to it (see Fig. 2). Correspondingly, the axes of the pick-up coils lie along the applied field direction in the present case. As the magnetized sample is driven with sinusoidal motion of frequency  $\omega$  and amplitude  $\zeta$  in the direction of the applied field (say the  $Z$  direction), a signal is induced in the (series-opposed) pick-up coils which is proportional to  $\zeta\omega(dB_z/dz)$ . Here  $B_z$  is the longitudinal component of the magnetic field of the sample, and the derivative is evaluated at the equilibrium position of the sample. When the coils are sufficiently remote from the specimen,  $(dB_z/dz)$  is proportional to  $M_{dz}$ , the magnetic dipole moment.

The assembly shown in Fig. 2 is immersed in liquid He except for the sample and sample drive-rod which are situated within an enclosed tubulation (not shown) containing a pressure of  $\approx 200 \mu$  of He gas which serves to maintain thermal equilibrium with the He bath.

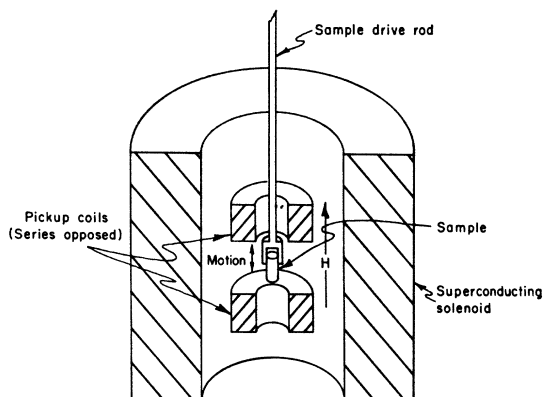


FIG. 2. Schematic of the experimental arrangement.

<sup>11</sup> R. R. Hake, Phys. Rev. **123**, 1986 (1961).

<sup>12</sup> R. R. Hake, D. H. Leslie, and T. G. Berlincourt, J. Phys. Chem. Solids **20**, 177 (1961).

<sup>13</sup> R. R. Hake, Phys. Rev. Letters **15**, 865 (1965).

<sup>14</sup> S. Foner, Rev. Sci. Instr. **30**, 548 (1959).

Temperatures are determined from the vapor pressure of the pumped He bath.

### Sample Preparation and Characterization

The basic sample preparation and characterization of Ti-Mo alloys has been described in detail elsewhere.<sup>11,12</sup> For the present purpose, the samples were cut from arc-case buttons and machined into the form of cylinders approximately 0.13 cm in radius by 1.0 cm long. The samples were then given an annealing treatment which consisted of one hour at 1440°C and then cooling at approximately 6°C/min. After annealing, the samples were chemically etched to remove possible surface inhomogeneities. Resistivity measurements were then made by a standard four-probe technique. In this way, the normal-state resistance and

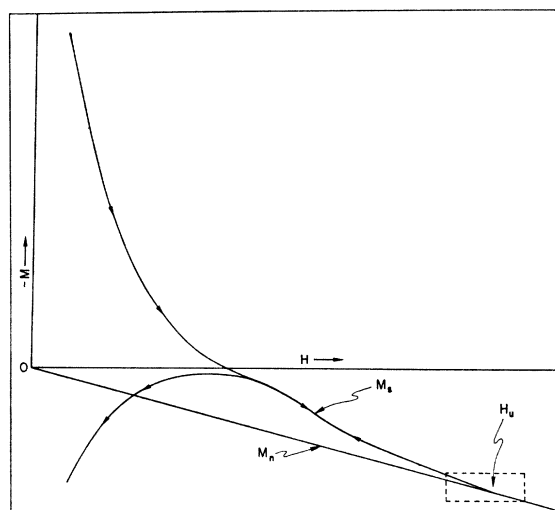


FIG. 3. A sketch of a typical magnetization curve for Ti-16 Mo. For clarity, the low-field region showing the Meissner state and  $H_{c1}$  has been omitted. Note how the magnetization becomes paramagnetic and joins the normal-state magnetization line  $M_n$  at the upper transition field  $H_u$ . The line  $\bar{M}_n$  is obtained from measurements at higher temperatures.

resistively determined superconducting transition temperature were measured. The resistivity at 4.2°K was  $103 \mu\Omega \text{ cm}$  and the transition temperature (onset of resistance) was 4.10°K,<sup>15</sup> in good agreement with the magnetically determined  $T_{c0}$  which is deduced by extrapolation of the critical-field curve.

The general features of an isothermal magnetization curve of the high- $\kappa$  "paramagnetically limited" superconductors have been described by Hake.<sup>13</sup> The present data are in general agreement with that description, although some additional features are evident. Figure 3 is a sketch from a recorder tracing of a typical mag-

<sup>15</sup> The exact transition temperature of Ti-16 at.% Mo is uncertain. For specimens machined from the same arc-cast button,  $T_c$  apparently varies somewhat perhaps due to inhomogeneities, annealing treatments, etc. Hake (Ref. 12) gives 4.18°K, and we have observed  $T_c$  (magnetic) as high as 4.23°K for a specimen from the same button.

netization curve as obtained by the vibrating sample magnetometer. It may be seen that the salient features are: (1) the initial flux penetration field  $H_{c1}$  is very small. This is typical of very high  $\kappa$  superconductors. (2) A substantial fraction of the magnetization curve lies below (or on the paramagnetic side of) the zero axis. This feature is a reflection of the fact that the mixed-state curve joins the normal state continuously, i.e. that (3), the transition to the normal state appears to be of second order.<sup>13</sup> Figure 4 illustrates the behavior of the magnetization near the transition field. One may note that  $M_s(H)$  appears to be linear near the transition field and that there is no evident discontinuity such as might accompany a first-order transition. (4) The magnetization curve exhibits a peculiar broad maximum over the middle portion of the mixed-phase region. (5) The magnetization curve is reversible over most of the paramagnetic region.

In the following, for clarity, we shall distinguish between the *measured* upper critical field  $H_u$  and the theoretical quantity  $H_{c2}$ . For the present purposes, we are interested in the temperature dependences of the upper transition field, and in the relative slope  $\chi_s = [\partial(M_n - M_s)/\partial H]_{H_u}$  of the magnetization curve at the upper transition field,  $H_u$  (see Fig. 4). Since the magnetization curves are reversible in the neighborhood of  $H_u$ , one expects that the values obtained for  $H_u$  and  $\chi_s$  from the present data should correspond to the equilibrium values described by the theory.

Curves such as that shown on Fig. 3 were taken at several temperatures between 1.9 and 4.1°K. From these, the critical fields  $H_u$  and the slopes at  $H_u$  were taken as the basic experimental data to be compared with theory.

#### COMPARISON OF EXPERIMENT AND THEORY

While the substance of the calculations of Maki<sup>8,9</sup> and of WHH<sup>10</sup> is the temperature dependence of  $H_{c2}$  for short mean free path ("dirty limit") superconductors, Maki<sup>9</sup> has also examined the situation in which an Abrikosov vortex lattice solution is fitted to the Gor'kov equations when the order parameter is small, i.e. near the transition field. He finds that the vortex lattice solution leads to results exactly analogous to the spin-independent case.<sup>16,17</sup> The result pertinent to our interest here is the magnetization, for which Maki gives

$$-4\pi(M_s - M_n) = (H_{c2} - H)/(2\kappa_2^2 - 1)\beta, \quad (1)$$

for  $(H_{c2} - H) \ll H_{c2}$ .

It will be noted that this formula is the same as that given for the spin-independent case<sup>16,17</sup> except that in the latter, the normal-state magnetization  $M_n$  is

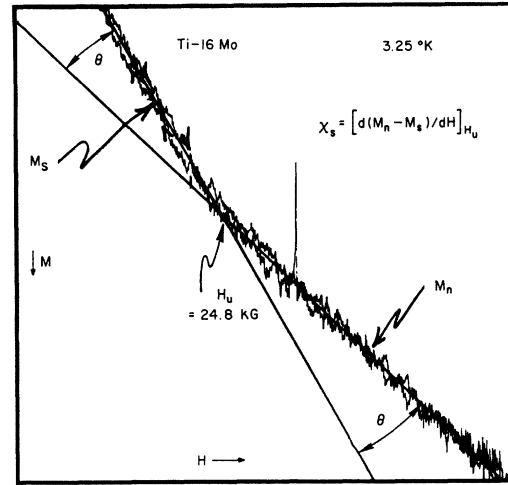


FIG. 4. Actual photograph of recorder tracing for the magnetization of Ti-16 at 3.25°K. This picture includes roughly the area enclosed in the dashed-line rectangle on Fig. 3. This figure illustrates the reversibility, and the apparent second-order character of the transition at  $H_u$ . The relative slope  $\chi_s$  is related to the Abrikosov-Maki parameter  $\kappa_2$  by  $\kappa_2 \approx (8\pi\beta\chi_s)^{-1/2}$ . See text.

deleted as it is considered to be negligible compared to the magnetization of the superconducting mixed phase. In the present case, on the other hand, a most obvious experimental feature is that the sample becomes *paramagnetic* well before the transition field  $H_u$  is reached (see Figs. 3, 4).

When electron spin and spin-orbit effects occur, the magnetization in (1) also differs from the spin-independent case in that the temperature dependences of  $H_{c2}$  and  $\kappa_2$  are substantially altered by the spin-dependent scattering effects. This is expressed formally in the following by the notation  $H_{c2} = H_{c2}(\alpha, \lambda_{so}, T)$ , and  $\kappa_2 = \kappa_2(\alpha, \lambda_{so}, T)$  where  $\alpha$ , the Pauli spin parameter, is effectively proportional to the normal-state Pauli spin susceptibility (proportional to the electronic density of states at the Fermi surface). It will be described further below. The parameter  $\lambda_{so}$  in the notation of WHH<sup>10</sup> is given by

$$\lambda_{so} = \hbar(3\pi k_B T_{c0} \tau_{so})^{-1}, \quad (2)$$

where  $\tau_{so}$  is the spin-orbit scattering time. Thus  $\lambda_{so}$  effectively measures the spin-orbit scattering strength. In the following, it enters as the only adjustable parameter in fitting the theoretical results to the experimental data.

In terms of the parameters  $\alpha$  and  $\lambda_{so}$ , the theoretical temperature dependence of the upper transition field is given by WHH<sup>10</sup> as

$$H_{c2}(\alpha, \lambda_{so}, T)/H_{c2}(0,0,0) = 2\gamma h, \quad (3)$$

where  $\gamma = \pi k_B T_{c0}/\Delta_{00}$ , and  $h(\alpha, \lambda_{so}, T)$  is given by the

<sup>16</sup> A. A. Abrikosov, Zh. Eksperim. i Teor. Fiz. 32, 1442 (1957) [English transl.: Soviet Phys.—JETP 5, 1174 (1957)].

<sup>17</sup> Kazumi Maki, Physics 1, 21 (1964).

solution of the Gor'kov equation

$$\ln 1/t = 2 \sum_{n \text{ odd}} \left\{ \frac{1}{n} - \left[ n + \frac{h}{t} + \frac{(\alpha h/t)^2}{n + (h + \lambda_{so})/t} \right]^{-1} \right\}, \quad (4)$$

where  $t = T/T_{c0}$ .

This calculation is expected to be valid in the approximation  $\tau_{tr} \ll \tau_{so}$ ; that is, when the spin-independent scattering predominates over spin-orbit scattering.

Maki<sup>9</sup> has derived Eq. (4), independently, and given a convenient approximate solution which is valid in the strong spin-orbit scattering limit. In the approximation

$$\tau_{so} \ll \hbar/\Delta_{00}, \quad (5)$$

Maki finds

$$h \simeq 2h_0 [1 + (1 + 2\delta h_0)^{1/2}]^{-1}, \quad (6)$$

where

$$h_0 \equiv \left( \frac{1}{2\gamma} \right) H_{c2}(0,0,t)/H_{c2}(0,0,0)$$

is the spin *independent* reduced critical field given by the Gor'kov equation

$$\ln 1/t = 2 \sum_{n \text{ odd}} \left\{ \frac{1}{n} - \frac{1}{n + h_0/t} \right\}, \quad (7)$$

and where

$$\delta \equiv \alpha^2/\lambda_{so}. \quad (8)$$

Thus, in Maki's solution,  $\alpha$  and  $\lambda_{so}$  enter only in the ratio given by  $\delta$ . By virtue of the BCS relation  $\xi_0 = \hbar v_F/\pi\Delta_{00}$  ( $\xi_0$  is the coherence length), the criterion (5) for the validity of this approximate solution is equivalent to  $\tau_{so} \ll (\pi\xi_0/l)\tau_{tr}$ . Thus, in the "dirty limit,"  $\xi_0/l \gg 1$ , one may have

$$\tau_{tr} \ll \tau_{so} \ll (\pi\xi_0/l)\tau_{tr}, \quad (9)$$

so that the criterion (5) is consistent with the criterion  $\tau_{tr} \ll \tau_{so}$  for the exact solution of Eq. (4).

### Experimental Results

In Fig. 5 are shown the present experimental data for the temperature dependence of the upper critical field  $H_u$ . (Our notation is  $H_u$  for experiment,  $H_{c2}$  for theory.) The center solid curve represents the theoretical prediction of WHH for  $\alpha = 1.75$  and  $\lambda_{so} = 0.7$  ( $\delta = 4.38$ ). Shown also for purposes of comparison are the curves for  $\alpha = 0, \lambda_{so} = 0$  (the expected upper transition field when no electron spin effects occur) and for  $\alpha = 1.75, \lambda_{so} = 0$  (when Pauli spin paramagnetism is included but spin-orbit scattering is neglected). The value of 1.75 for  $\alpha$  is not arbitrary, but is given by the electronic structure parameters of Ti-16 at.% Mo (see the next section). The fact that the experimental data fall well above the curve for  $\alpha = 1.75, \lambda_{so} = 0$  suggests that spin-orbit scattering plays a substantial role in determining the critical field of Ti-16 at.% Mo. It seems worthy of emphasis that the theoretical curve not only fits the qualitative features of the experimental results, but, in fact, with a single adjustable

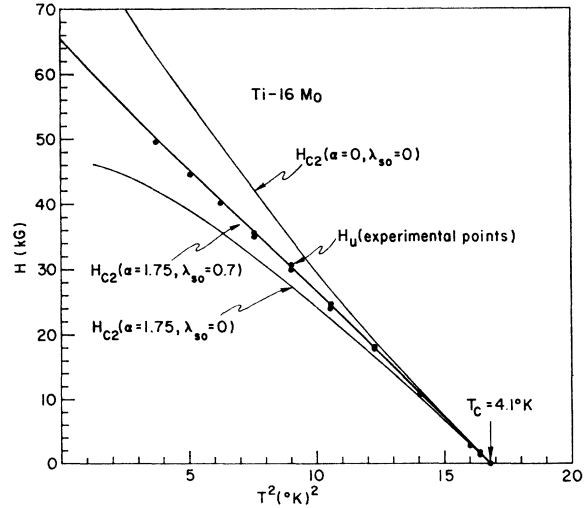


FIG. 5. The measured upper critical field  $H_u$  for Ti-16 at.% Mo (data points) and the theoretical critical field  $H_{c2}$  (solid lines) for three sets of values of the Pauli spin parameter  $\alpha$ , and the spin-orbit parameter  $\lambda_{so}$ . With  $\alpha = 1.75$  (given by specific-heat and normal-state-resistance data), the value of  $\lambda_{so}$  is the only adjustable parameter. Note that the theoretical curve for  $\lambda_{so} = 0.7$  displays the unusual inflection which is suggested by the data points.

parameter, gives a remarkably accurate numerical value for the upper critical field over a fairly wide temperature range. Note that even the inflection in the curve of the experimental data is found in the theoretical curve. The curve given by Maki's approximate solution, Eqs. (5) and (6), is not shown on Fig. 5, but is compared with the exact solution and the experimental data on Fig. 6 where we have plotted the quantity

$$\Delta H = H_{c2}(\alpha, \lambda_{so}, T) - (4\gamma/\pi^2) H_{c2}(0,0,0)(1 - t^2). \quad (10)$$

The last term represents a parabolic curve with the same slope at  $T_{c0}$  as the theoretical curve for  $H_{c2}(\alpha, \lambda_{so}, T)$ . Hence  $\Delta H$  is directly amenable to calculation. This procedure has the advantage that the actual predicted value at  $T=0$  (WHH  $\rightarrow$  65.5 kG, Maki  $\rightarrow$  66.7 kG) is not obscured. One notes that either curve, but not both, can be brought into very close agreement with the data by an appropriate change in  $\lambda_{so}$ . It turns out that a 10% change in  $\tau_{so}$  produces roughly a 5% change in  $H_{c2}(T)$  near  $t=0$ . At higher temperatures the change becomes less sensitive. One may conclude therefore that for the present range of parameters and for  $t \gtrsim 0.5$ , Maki's approximate solution for Eq. (3) may be fitted to the experimental data with an error (relative to the exact solution) in  $\tau_{so}$  not exceeding  $\approx 10\%$ .

The temperature dependence of  $\kappa_2$  is shown on Fig. 7. The experimental points were obtained from the measured change in slope at  $H_u$ , by using formula (1) (see Fig. 4). The theoretical curves shown here are drawn from Maki's recent calculations.<sup>9</sup> Here, Maki's parameter  $\delta$  is related to the WHH<sup>10</sup> spin-orbit scatter-

ing parameter by Eq. (8). For the present chosen values,  $\alpha=1.75$ ,  $\lambda_{so}=0.7$ , one has  $\delta=4.38$  as shown on the figure. The experimental data points run somewhat higher than the corresponding theoretical curve. The data points shown represent averages taken from several runs and for this reason exhibit no appreciable scatter. It is difficult, however, to assess accurately the possible *systematic* limits of error for the experimental values. For example, to compute the ratio  $\kappa_2(t)/\kappa_2(1)$ , one first obtains  $\kappa_2(t \rightarrow 1)$  by extrapolation. The result obtained (see Fig. 6) is 65 with an estimated accuracy of  $\pm 5$ . This factor alone can produce a uniform error of nearly 10% in the ratio  $\kappa_2(t)/\kappa_2(1)$ . Thus, we cannot at present exclude the possibility that the discrepancy between the data and theory is within the range of systematic experimental error.

On the other hand, the qualitative agreement is quite satisfactory. For example, for nonparamagnetic superconductors,  $\kappa_2$  is observed to increase with decreasing temperature<sup>9,18</sup> as predicted by the theory, and conversely, for the paramagnetic specimen studied here,  $\kappa_2$  is observed to decrease with decreasing temperature as predicted.

The curve for  $\kappa_2(\lambda_{so}=0)$  actually leads to a value of zero for  $\kappa_2$  at finite temperatures ( $\beta^2 \approx 0.2$ ). For this reason, Maki earlier<sup>8</sup> concluded that a 1st order transition ( $\chi_s \rightarrow \infty$ ) should occur for superconductors with a large Pauli term, i.e.,  $\alpha \gtrsim 1$ . In view of the present data where  $\alpha > 1$ , this conclusion appears unlikely unless there should occur very weak spin-orbit scattering in some superconductors which have a large Pauli term.

#### COLLECTED THEORETICAL FORMULAS AND EXPERIMENTAL VALUES

The following is a compendium of useful theoretical formulas and numerical values appropriate to the present experiments and providing further comparison with the theory.

##### The Pauli Spin Parameter

$$\equiv 3\hbar/2mlv_F = 3e^2\hbar\rho_n\gamma_c/2m\pi^2k_B^2 = 2.36 \times 10^{-6}\rho_n\gamma_c. \quad (11)$$

In (11),  $l$  is the mean free path, and  $v_F$  the Fermi velocity. The second and third equalities follow from the free-electron model where  $\rho_n$  is the normal-state resistivity in  $\mu\Omega$  cm and  $\gamma_c$  is the electronic-specific-heat coefficient in  $\text{ergs cm}^{-3} \text{ }^\circ\text{K}^{-2}$ . Using the values  $\rho_n=103$  (measured) and  $\gamma_c=7.3 \times 10^3$  [Ref. (13)], one finds  $\alpha=1.77$  for Ti-16 at % Mo.

##### The Upper Critical Field

We have used the notation  $H_u$  for the measured upper transition field and  $H_{c2}(\alpha, \lambda_{so}, T)$  for the theo-

<sup>18</sup> In an earlier publication, Maki (Ref. 17) reported that  $\kappa_2(0,0,T)$  decreased with decreasing temperature. He has since discovered an error in those calculations and the corrected results are those shown in Fig. 7. The new results are in good agreement with experiments by the author on V-5% Ta (to be published).

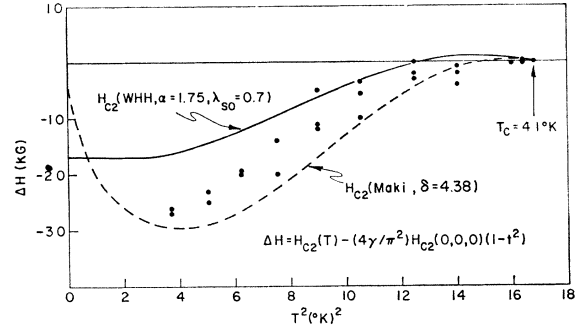


FIG. 6. Plot of the function  $\Delta H = H_{c2} - (4\gamma/\pi^2)H_{c2}(0,0,0)(1-\beta^2)$ . The dashed line is obtained when  $H_{c2}$  is Maki's  $H_{c2}(\delta, T)$ ; the solid line for  $H_{c2}(\alpha, \lambda_{so}, T)$  after Werthamer *et al.* (Ref. 10), and the points are obtained when the experimental values  $H_u$  (Fig. 5) are used for  $H_{c2}$ . Here  $\gamma = \pi k_B T_{c0}/\Delta_{00}$ , so the quadratic term represents a hypothetical parabolic critical field which has the theoretically expected slope at  $T_{c0}$ .

retical critical field. At  $T=0^\circ\text{K}$ , the theory gives:

$$H_{c2}(0,0,0) = 3\Delta_{00}/2elv_F = 3.09 \times 10^{-2}\rho_n\gamma_c T_{c0} = 1.31 \times 10^4 \alpha T_{c0}, \quad (12)$$

where we have used the BCS<sup>19</sup> relation

$$\gamma = \pi k_B T_{c0}/\Delta_{00} = e^C C_E = 1.781, \quad (13)$$

where  $C_E=0.5772$  is Euler's constant.

For the present alloy, the electronic structure parameters give  $H_{c2}(0,0,0)=95.3$  kG, much larger than the observed (extrapolated) value of  $H_u(0) \approx 65$  kG.

##### The Slope of the Critical-Field Curve at $T_c$

$$\begin{aligned} & \left[ \frac{dH_{c2}(\alpha, \lambda_{so}, T)}{dT} \right]_{T_{c0}} \\ &= \left[ \frac{dH_{c2}(0,0,T)}{dT} \right]_{T_{c0}} = 12k_B/\pi elv_F \\ &= (8\gamma/\pi^2 T_{c0}) H_{c2}(0,0,0). \end{aligned} \quad (14)$$

Combining with (12) and (13), one has

$$\alpha = (\pi\mu_B T_{c0}/2k_B) (dH_{c2}/dT^2)_{T_{c0}} = 1.05 \times 10^{-4} T_{c0} (dH_u/dT^2)_{T_{c0}}. \quad (15)$$

Thus,  $\alpha$  can be determined from the slope of the observed critical-field curve when the specific-heat coefficient  $\gamma_c$  is *not* known. For the present case (see Fig. 5), we find  $(dH_u/dT^2)_{T_{c0}} \approx 4.0 \times 10^3$  which gives  $\alpha=1.72$  in good agreement with the value given by (11). A value of  $\gamma_c$  can now be calculated. One obtains  $7.1 \times 10^3 \text{ erg cm}^{-3} \text{ }^\circ\text{K}^{-2}$ .

##### The Gor'kov Parameter $\kappa_G$

The parameter  $\kappa_G$  is defined to be<sup>5</sup>

$$\kappa_G = (3\hbar^2/2\pi^2 e\tau m v_F^2) \times [2\pi\zeta(3)\hbar/v_F]^{1/2} = 7.5 \times 10^{-3}\rho_n\gamma_c^{1/2} \quad (16)$$

$$= 31.8\alpha\gamma_c^{-1/2}. \quad (17)$$

<sup>19</sup> J. Bardeen, L. N. Cooper, and J. R. Schrieffer, Phys. Rev. **108**, 1175 (1957).

If  $\gamma_c$  is unknown,

$$\kappa_G = 4.88\alpha^{1/2}\rho_n^{1/2}. \quad (18)$$

For Ti-16 at. % Mo, using  $\rho_n = 103$ ,  $\gamma_c = 7300$ , one finds  $\kappa_G = 66$ . Maki's theory predicts that

$$\kappa_G = \kappa_1(\alpha, \lambda_{s0}, T_{c0}) \quad (19)$$

$$= \kappa_2(\alpha, \lambda_{s0}, T_{c0}). \quad (20)$$

Thus, it is possible to check further the theory by determining  $\kappa_2(\alpha, \lambda, T)$  and  $\kappa_1(\alpha, \lambda, T)$  from the magnetic measurements, and extrapolating to the limit  $T = T_{c0}$ .

The  $\kappa_2$  values are obtained from the slope of the magnetization curve according to

$$\kappa_2(\alpha, \lambda_{s0}, T) \simeq (8\pi\beta\chi_s)^{-1/2}, \quad (21)$$

where

$$\chi_s = [d(M_n - M_s)/dH]_{H_u}, \quad (22)$$

and for  $\beta$ , we have used the value of 1.16 appropriate to the triangular<sup>20</sup> vortex lattice.

For the present alloy, we find  $\kappa_2(T \rightarrow T_{c0}) \approx 65 \pm 5$  in excellent agreement with the value given by the Gor'kov-Goodman formula (16).

The parameter  $\kappa_1(T)$  is defined by the well-known relation

$$\kappa_1 = H_{c2}/\sqrt{2}H_c, \quad (23)$$

where  $H_c$  is defined by the relation

$$H_c^2/8\pi = \int_0^\infty (M_n - M_s)dH, \quad (24)$$

and the right-hand side is just the area between the

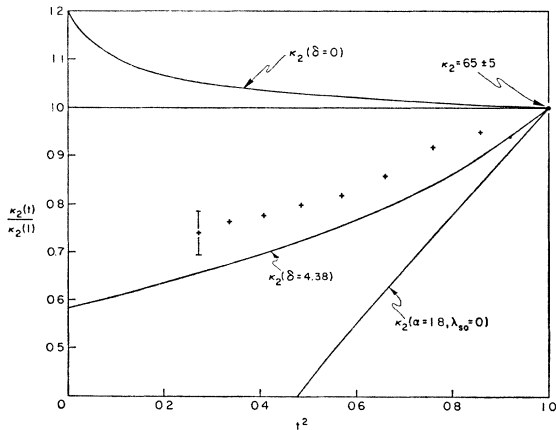


FIG. 7. The Abrikosov-Maki parameter  $\kappa_2(\alpha, \lambda_{s0}, T)$ . The experimental points are obtained from the Abrikosov formula [Eq. (21) of text] from the relative slope  $\chi_s$  of the magnetization curve at  $H_u$  (see Fig. 4). The theoretical curves, after the recent theory of Maki, are drawn for the case of no spin effects (top curve) and for various values of the spin parameters.

<sup>20</sup> D. Cribier, B. Jacrot, B. Farnoux, and L. Madhav Rao, J. Appl. Phys. **37**, 952 (1966); in *Proceedings of the Ninth International Conference on Low Temperature Physics*, edited by J. G. Daunt, D. O. Edwards, F. J. Milford, and M. Yaqub (Plenum Press, Inc., New York, 1965), p. 513.

normal and superconducting magnetization curves (see Fig. 3).

Unfortunately, we have not been able to obtain reasonable values of  $H_c$  from the experimental areas. The curves of Fig. 3 show a good deal of irreversibility below about  $H_u/2$ , and it was found that if at any time the field sweep was halted on the down sweep cycle, the signal would then gradually drift towards the upsweep curve, usually ending not farther than  $\approx 10\%$  below the upsweep curve. This suggested that the upsweep curve (which was stable in stationary fields) was close to the equilibrium curve.

However, the areas under the upsweep curves were invariably too large, i.e. gave  $H_c$  values nearly twice as large as the BCS values. This result could be a peculiarity of the vibrating-sample magnetometer (perhaps because of the inhomogeneous magnetic field) or some intrinsic complication in the behavior of paramagnetically limited superconductors. While the problem needs further study, it does not compromise the results discussed above which are based on data obtained in the reversible region above  $\sim H_u/2$ .

It is perhaps noteworthy, however, that the temperature dependence of the observed area was such as to be in good agreement with the BCS<sup>19</sup> theory. This is shown in Fig. 8. Accordingly, one may undertake to use the BCS<sup>19</sup> values for  $H_c(T)$  and compare the values thus obtained for  $\kappa_1(T_{c0})$  with the Gor'kov-Goodman value of 66. Near  $T = T_{c0}$ , one has

$$\kappa_1(\alpha, \lambda_{s0}, T_{c0}) = (dH_u/dT)_{T_{c0}}/\sqrt{2}(dH_c/dT)_{T_{c0}}. \quad (25)$$

Using for  $(dH_u/dT)_{T_{c0}}$  the experimental value of  $\sim 3.3 \times 10^4$  and for  $(dH_c/dT)_{T_{c0}}$ , the BCS<sup>19</sup> value  $(19.4\gamma_c)^{1/2}$ , we obtain  $\kappa_1(T_{c0}) = 61$ , in good agreement with the Gor'kov-Goodman value.

## CONCLUSIONS

The alloy Ti-16 at. % Mo appears to be a "paramagnetically limited superconductor" in that its upper critical field is influenced by electron spin effects. From the foregoing comparison of experimental and theoretical results, the following conclusions appear to be warranted.

(1) The temperature dependence of the upper critical field of Ti-16 at. % Mo is accurately predicted by recent theories when both Pauli-spin paramagnetism and spin-orbit scattering are taken into account. An adequate fit of theory and experiment is not possible if spin-orbit scattering is neglected.

(2) Good quantitative agreement between theory and experiment is obtained when numerical values derived from the weak-coupling limit of the microscopic theory are used [e.g.,  $\Delta_{00}/k_B T_{c0} = 1.76$ ,  $H_c(0)/\gamma_c^{1/2} T_{c0} = 2.44$ ].

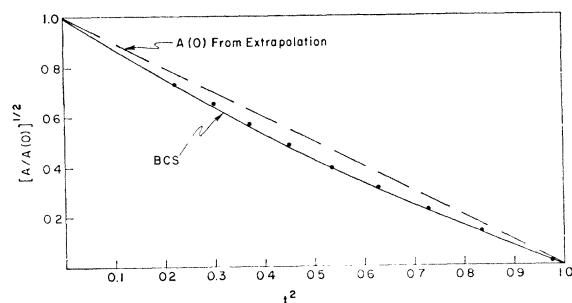


FIG. 8. Plot of the normalized square root of the measured area enclosed between the superconducting- and normal-state magnetization curves versus the square of the reduced temperature  $t = T/T_{c0}$ . These areas are for superconducting curves taken in increasing fields (see Fig. 3). For ideally reversible curves the ordinate is expected to be proportional to the "thermodynamic critical field"  $H_c$ . These results are thought to be consistent with the view that the  $H_c$  values are not appreciably altered by spin effects.

(3) The behavior of the magnetization of Ti-16 at. % Mo in the vicinity of the upper critical field suggests that the transition to the normal state is of second

order with a finite change in slope at the transition point. The change in slope is related to the electronic structure and the spin and spin-orbit effects by an expression which is a generalization due to Maki of Abrikosov's formula for the spin-independent case. The fair agreement between theory and experiment for the slope of the magnetization curve suggests that Abrikosov's vortex lattice solution may be an appropriate description of the magnetic structure even when spin effects are substantial.

#### ACKNOWLEDGMENTS

Special thanks are owed to D. H. Leslie for his excellent technical assistance in developing the apparatus and acquiring the data. I wish to thank K. Maki for the pre-publication use of his calculations, and finally I wish to acknowledge helpful discussions with T. G. Berlincourt at whose suggestion this study was undertaken.

### Strong-Coupling Superconductivity. I\*

D. J. SCALAPINO†, J. R. SCHRIEFFER, AND J. W. WILKINS‡

*Department of Physics, University of Pennsylvania, Philadelphia, Pennsylvania*

(Received 16 February 1966)

The pairing theory of superconductivity is extended to treat systems having strong electron-phonon coupling. In this regime the Landau quasiparticle approximation is invalid. In the theory we treat phonon and Coulomb interactions on the same basis and carry out the analysis using the nonzero-temperature Green's functions of the Nambu formalism. The generalized energy-gap equation thus obtained is solved (at  $T = 0^\circ\text{K}$ ) for a model which closely represents lead and the complex energy-gap parameter  $\Delta(\omega)$  is plotted as a function of energy for several choices of phonon and Coulomb interaction strengths. An expression for the single-particle tunneling density of states is derived, which, when combined with  $\Delta(\omega)$ , gives excellent agreement with experiment, if the phonon interaction strength is chosen to give the observed energy gap  $\Delta_0$  at zero temperature. The tunneling experiments therefore give a detailed justification of the phonon mechanism of superconductivity and of the validity of the strong-coupling theory. In addition, by combining theory and the tunneling experiments, much can be learned about the electron-phonon interaction and the phonon density of states. The theory is accurate to terms of order the square root of the electron-ion mass ratio,  $\sim 10^{-2}$ – $10^{-3}$ .

#### I. INTRODUCTION

IN the original BCS theory of superconductivity,<sup>1</sup> a central role was played by the concepts provided by Landau's theory of a Fermi liquid.<sup>2</sup> In Landau's theory,

\* This work was supported in part by the National Science Foundation and by the Laboratory for Research on the Structure of Matter, University of Pennsylvania, covering research sponsored by the Advanced Research Projects Agency. Part of the work reported here was performed as a portion of a thesis of one of us (J.W.W.) in partial fulfillment of the requirement for a Ph.D. degree in Physics, University of Illinois, 1963.

† Alfred P. Sloan Foundation Fellow.

‡ Present address: Department of Physics, Cornell University, Ithaca, New York.

<sup>1</sup> J. Bardeen, L. N. Cooper, and J. R. Schrieffer, *Phys. Rev.* **108**, 1175 (1957).

<sup>2</sup> L. D. Landau, *Zh. Eksperim. i Teor. Fiz.* **30**, 1058 (1956).

the excited states  $\Phi_N$  of the Fermi liquid are placed in one-to-one correspondence with the excited states of a free Fermi gas. That is, the excited states  $\Phi_N$  are labelled by the occupation numbers  $\nu_{ks}$  of the "quasi-particle" states of momentum  $\mathbf{k}$  and spin component  $s$  ( $\uparrow$  or  $\downarrow$ ) in analogy with single particle occupation numbers  $n_{ks}$  of the free Fermi gas. Presumably the Landau configurations  $\Phi_N$  contain most of the many-body correlations occurring in the superconducting energy eigenfunctions  $\Psi_s$  except for those correlations which are specific to the superconducting phase, i.e., the pairing correlations.

Since the states  $\Phi_N$  form a complete set, a state  $\Psi_s$